IL NUOVO CIMENTO Vol. 26 C, N. 5 Settembre-Ottobre 2003
DOI 10.1393/ncc/i2003-10005-9

Northern Adriatic general circulation behaviour induced by heat fluxes variations due to possible climatic changes

A. Bergamasco([1])([*]), V. Filipetto([1]), A. Tomasin([2]) and S. Carniel([1])

([1]) *CNR-ISMAR - S. Polo 1364, I-30125 Venezia, Italy*

([2]) *Dipartimento di Matematica Applicata, Università di Venezia*
Dorsoduro 3825, I-30123 Venezia, Italy

(ricevuto il 17 Febbraio 2003; revisionato il 6 Novembre 2003; approvato il 19 Novembre 2003)

Summary. — The thermohaline circulation of the central-north Adriatic basin is investigated by means of a 3D hydrodynamic numerical model. Three different runs —where the surface heat fluxes annual average is respectively negative, slightly positive and slightly negative—are performed; the general circulation patterns are then discussed and depicted, also with the aid of the trajectories of numerical particles released during the integrations. Results confirm that surface heat fluxes can start and trigger the general circulation in the basin (both vertically and horizontally), even without prescribing other forcings. Particularly, when the annual budget of the heat fluxes is negative (*i.e.* the basin loses heat to the atmosphere) a horizontal cyclonic surface circulation is generated, characterized by a northward flow along the eastern coast and a southward return current system along the western one. From the vertical point of view, an antiestuarine circulation is established. A similar circulation pattern is depicted when the surface fluxes have a slightly negative annual budget. On the other hand, when the annual fluxes balance is positive the vertical circulation switches to estuarine and, as expected, the integrated circulation becomes anticyclonic. A modification in the heat fluxes budget is strictly related to a change in the water column turnover time of the Jabuka pit, the deepest meso-Adriatic depression: when the annual heat fluxes balance is negative but close to zero, the dense-water residence time in the pit becomes minimum and the water has a shorter turnover time, denoting a faster renewal compared to those exhibited in the other experiments.

PACS `92.10.-c` – Physics of the oceans.
PACS `92.70.-j` – Global change.

([*]) E-mail: andrea.bergamasco@ismar.cnr.it

1. – Introduction

In the past centuries several periodic cycles or fluctuations interested the Earth climatic conditions [1, 2]; according to IPCC [3], particularly relevant climatic changes due both to natural events and to human activities seem to be occurring in the last few decades. Among them, the relation between global warming and the ocean general circulation is probably one of the most important and yet not completely understood. Several authors, indeed, stress the possibility that climatic changes may interfere with—and possibly reverse—some of the global and regional ocean circulation features as the Gulf current, the Antarctic Circumpolar Current, etc. [4-7].

This would induce modifications in the distribution of quantities as heat or nutrients: the effects—due to high non-linear relations and complex feedback mechanisms—are largely unknown and could therefore generate concern for the environment in future scenarios [8-10].

Many uncertainties arise when trying to depict the long-term effects of the thermal forcing on oceans, mostly due to systematic errors and natural climatic variabilities [11]. However, the assessment and quantification of its consequences over broad spatial and temporal scales is one of the most urgent questions that the international scientific community is requested to answer.

The aim of this paper is to investigate how the atmosphere-ocean interactions vary according to a modification—which may be induced by climatic change processes—of thermal forcings. The objective of the work is posed on the effects that different heat fluxes may have on the formation and evolution of the northern Adriatic Sea circulation, a broad shallow region (fig. 1) where important processes of dense-water formation occur [12-14].

More specifically, by using a 3D numerical hydrodynamic model, different scenarios are simulated in order to explore the sensitivity of the heat fluxes-generated thermohaline circulation and of the water turnover time of the meso-Adriatic depression (Jabuka pit, see fig. 1).

Other driving circulation forcings, like bora or sirocco winds, are not included in the model since they generally influence the basin-scale circulation for limited and short temporal scales. Moreover, even though rivers discharge may affect the hydrological cycle and also play a role in the long-term basin circulation, in the present study they have been omitted, since the focus is on the heat fluxes variations.

The paper is outlined as follows: Sect. **2** presents the description of the numerical model and the numerical experiments carried out; results and discussions are given in sect. **3**, while conclusions are drawn in sect. **4**.

2. – Model description and numerical experiments

The numerical model used in this work is the Princeton Ocean Model (POM) in the 1997 version [15]. It is a three-dimensional, free-surface model for an incompressible, Boussinesq and hydrostatic fluid resolving non-linear and time-dependent primitive equations. The model reproduces the sea surface elevation, the velocity fields and the space-time evolution of temperature and salinity. The turbolence closure scheme proposed by Mellor and Yamada and known as "level $2^1/_2$" [16] is adopted for the parameterisation of vertical mixing. In the past decades, the POM has been extensively used by several authors and proved to be one of the most powerful tools available for hydrodynamic

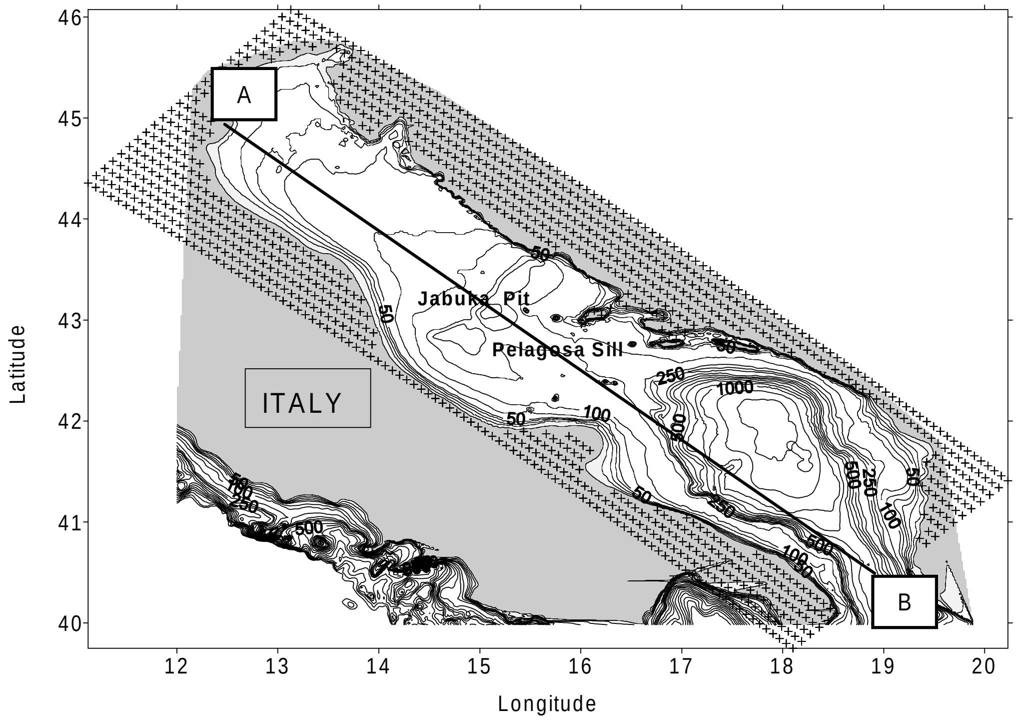

Fig. 1. – Bathymetry of the Adriatic Sea and numerical grid used in the model. Crosses represent the land points.

investigations in the Adriatic area, both for transient situations [17] and climatological applications [18].

In this work the POM has been implemented for the Adriatic Sea, using a bathymetry obtained by averaging and smoothing [19] original data from Naval Oceanographic Database. The grid, consisting in 25 × 100 points and rotated anti-clockwise by 47° from the parallel axis (see again fig. 1), has a coarse horizontal resolution (10.5 km in the transverse direction and 7.7 km in the axial one) and a relatively high vertical one: 35 sigma levels are used with a logarithmic distribution at the surface and bottom layers, in order to describe the deep-water formation processes and the dense-water dispersion more properly. In this way, while the coarse horizontal resolution is not affecting the main scientific goal of the work, the high vertical resolution allows, in ther northern Adriatic region, to describe the water column spanning from few centimetres to few meters.

Along the open boundary, located in the south region close to the Otranto Strait, the tidal component M_2 (28.9841 degree/h) is imposed, using 7.2 cm as amplitude, in agreement with previous studies and tide-gauge measurements carried out in the region (*e.g.* [20]). A radiation condition is applied for temperature and salinity fields with a relaxation time of about two hours; this allows the system to evolve inside the domain and radiate outside through the boundary both temperature and salinity values.

2˙1. *Initial conditions and physical forcings.* – Being the study process oriented, the model is initialized with horizontally uniform temperature and salinity profiles. Vertically, a typical stratification is assumed, with a thermocline set at a depth between 20

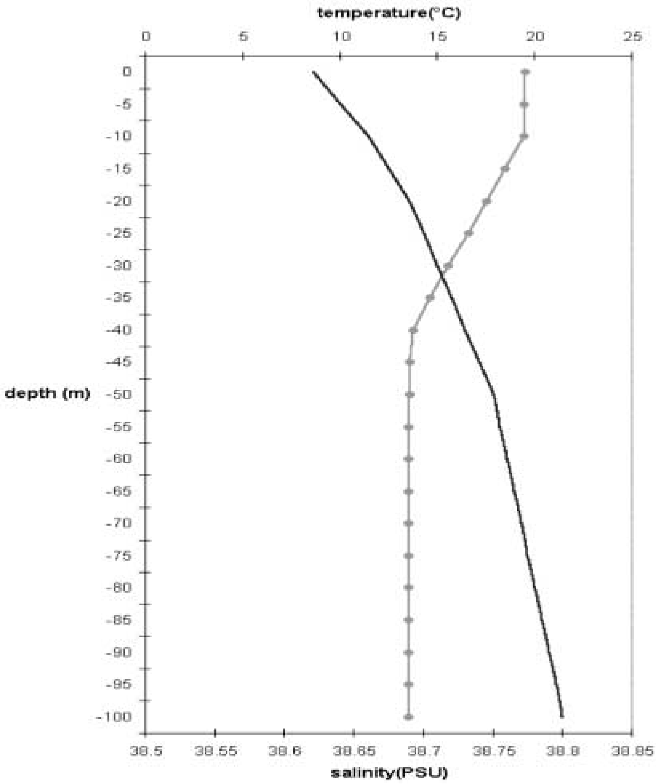

Fig. 2. – Initial temperature (dotted) and salinity profiles used in the model. Values below shown depths are equal to those at 100 m.

and 30 m (similar to the case proposed by [21]); initial temperature and salinity profiles are shown in fig. 2. Values below 100 m depths are equal to those at 100 m.

The basin is first spin up for 30 days only with M_2 tide imposed at the open boundary for geostrophic adjustment of the domain, then a five-years numerical integration is carried out, using the same forcings as perpetual. The heat fluxes are imposed in the northern/central Adriatic Sea with the maximum intensity at the centre on the northern basin, idealizing a spatial distribution derived from the climatology of May [22, 23] and summarized in table I. This simulates a winter cooling and a spring-summer heating. Even if the values, changing on a monthly base, are different in each experiment, all the runs are characterized by a seasonal cycle with a maximum heat loss in January-February and a maximum heat gain in the period between June and July. The values and the seasonal cycle adopted are in agreement with studies made by Stravisi and Crisciani [24], Picco [25] and Artegiani *et al.* [14].

As stated in the Introduction, other forcings as wind stress and river runoff are not included, their influence on the basin circulation being not the main objective of the present work.

2˙2. *Numerical experiments*. – Three numerical experiments are carried out. In Run 1 the maximum cooling of 100 W/m^2 is reached in January and February, while the max-

TABLE I. – *Monthly surface heat fluxes. All units are in* W/m^2.

Month	Sep.	Oct.	Nov.	Dec.	Jan.	Feb.	Mar.	Apr.	May.	Jun.	July	Aug.	Annual average
Run 1	−20	−40	−60	−80	−100	−100	0	20	30	50	40	0	−21.60
Run 2	10	−10	−30	−50	−70	−70	30	50	60	80	70	30	+8.3
Run 3	−20	−40	−60	−80	−100	−100	10	40	60	100	80	20	−7.5

imum heating of 50 W/m^2 is reached in June (see table I). The annual heat budget is negative (-21.6 W/m^2), as estimated by several authors [13, 25].

In Run 2 the annual heat balance is slightly positive, 8.3 W/m^2. All the fluxes are shifted toward positive values and the winter heat balance is smaller (in absolute value) than the spring one.

In Run 3 the winter fluxes are the same of Run 1, but the spring fluxes are higher (see again table I); the annual heat budget is slightly negative -7.5 W/m^2. During the numerical integration, fluxes change their values on the first day of each month.

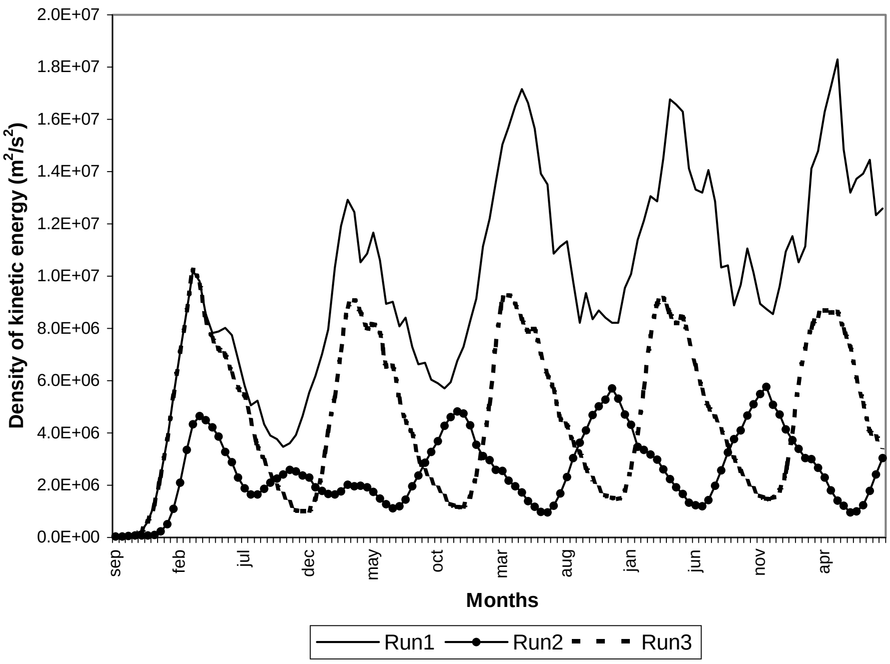

Fig. 3. – Kinetic-energy density trend. The values are expressed per unit of mass (m^2/s^2). Run 1 values are higher and increase every year. In Run 2 a steady-state condition is reached in three years, while in Run 3 in about two years.

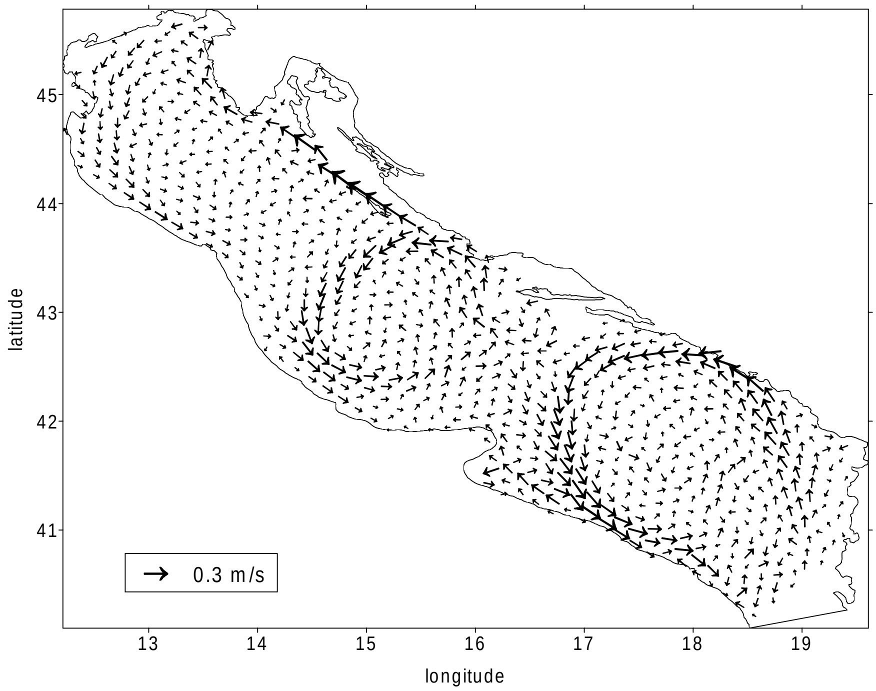

Fig. 4. – Surface velocity circulation pattern (Run 1, average relative to the last 15 days of January).

3. – Results and discussion

For the northern and central basin (where fluxes force the system) the average kinetic energy (KE) trend is computed and presented in fig. 3.

Before going into details of the resulting circulations, we can here summarize that in Run 1 the KE value increases during the first three years, after which the system reaches a quasi-steady condition. In Run 3 the average kinetic energy reaches a steady state in two years, while the trend of the first year is similar to that exhibited during Run 1, and during the following years it decreases because of the different fluxes. In Run 2, the average trend of the kinetic energy appears variable during the three years, denoting a transient behaviour that remains visible when a steady state is reached. It is interesting to note a phase-difference of kinetic energy between Run 1, Run 3 and Run 2. While in the former ones (with negative annual heat fluxes balance) the KE values are maximum during summer, during Run 2, characterized by a positive annual budget of heat fluxes, KE maximum is reached during winter.

3˙1. *Horizontal and vertical circulation.* – Figure 4 presents the average horizontal circulation as reproduced by Run 1: a cyclonic circulation pattern is generated (in accord with previous studies, *e.g.*, Orlic *et al.* [26]) and the circulation is characterized by two main gyres situated over the southern deep basin and the central one. The mean surface velocity (corresponding to the model uppermost sigma level) is bracketed between 0.12–0.16 m/s. A northward flow along the eastern coast and a southward current along the western one describe a cyclonic circulation in the shallow northern region as well, as

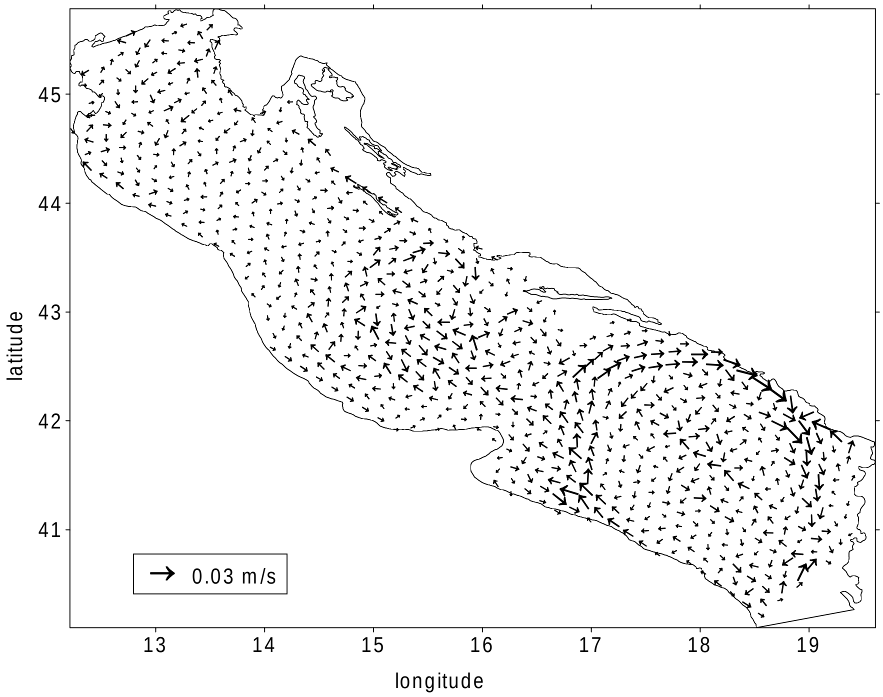

Fig. 5. – Surface velocity circulation pattern (Run 2, average relative to the last 15 days of January).

described also by Orlic *et al.* [26] and Artegiani *et al.* [13,14]. A general circulation, with similar features even if characterized by a less intense velocity field, is observed when analyzing Run 3 results (not presented here). Figure 5 shows the patterns resulting from Run 2: an anticyclonic circulation with a mean surface velocity one order of magnitude less than that reproduced in Run 1 (0.03–0.04 m/s) is evident.

The main circulation features of Run 1 are depicted and further investigated using also a numerical Lagrangian technique [27] where numerical particles are "released" in the basin and their resulting positions allow a comparison with experimental drifter measurements [28, 29]. The numerical particles are released from December (when the basin is forced by a heat loss of 80 W/m^2) to March, when the heat gain period starts, especially on the northern region where surface heat fluxes are maximum and the mass formation processes occur. The particles are released inside each grid when the surface density anomaly is greater than 28.3 kg/m^3, and are tracked for a whole year of integration. Besides advection effects, the Lagrangian simulation accounts also for a random walk diffusion proportional to the horizontal turbulent diffusivities modeled by the hydrodynamic module. At the end of the year, a total of 7583 particles out of 9519 initially released are still active and present in the water column; some of the remaining particles are deposited by the circulation on the domain closed boundaries, and part of them on the bottom, especially on the Pelagosa sill and along the Italian coast south of the Gargano Peninsula, which may probably represent areas with a strong vertical activity.

Thus, the numerical drifters mainly describe the behaviour of the dense-water masses formed in the northern region, flowing southward along the Italian coastline and showing

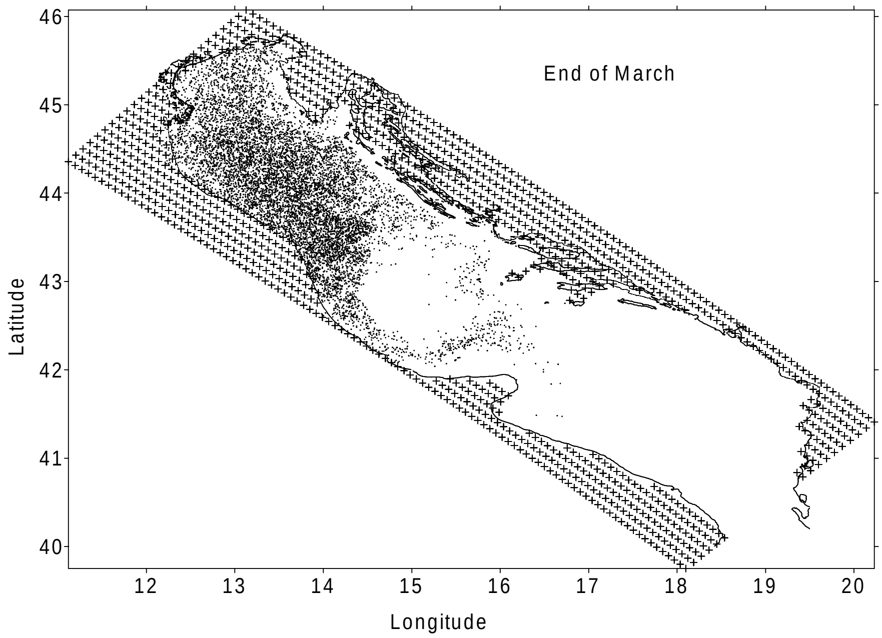

Fig. 6. – Position of all active drifters at the end of March of the first year (Run 1). A water flow directed southward along the Italian coastline is evident. Crosses represent the land points.

then the characteristic branch of the western cyclonic circulation, a cyclonic gyre over the central basin and a northward flow along the east coast. Some particles captured in the central gyre then flow further south reaching—and sometimes crossing—the Pelagosa sill. While during the winter period the particles remain mostly confined to a coastal boundary layer (fig. 6), in summertime they are spread in all the central basin.

Some of the drifter trajectories are describing the characteristic cyclonic circulation behaviour established in Run 1. As an example, in fig. 7 three drifters tracks are presented: particle "A", released in December, shows an isolated behaviour in the Northern Adriatic [30] maybe due to the weaker circulation and the heat fluxes distribution imposed. In fact "A" flows from the side of release towards the east coast, then it meanders in the north region where remains confined. The cyclonic circulation on the central and northern basin is highlighted (in accord with Orlic *et al.* [26] and Artegiani *et al.* [13,14]) by the path of the "B" and "C" particles, released in January and December, respectively. Particle "B" flows southward along the Italian coast where it is captured by the cyclonic central gyre and after 188 days (in July) reaches the southern basin crossing the Pelagosa sill, while particle "C", after a wide cyclonic gyre in the northern basin, moves southward along the western coast, reaching the central basin and then the Pelagosa sill.

It is evident from the numerical particles that the heat fluxes influence the horizontal Adriatic circulation; two characteristic gyres are evidenced in the shallow northern region and in the central basin, where the numerical drifters are looped in. In the central basin, particles round mostly on the border of the gyre and only part of them spreads inside during the summer time. Experimentally, it has been observed that the sub-basin circulations are connected and at the same time independent [30]: some particles in fact remain on the central basin, while some others leave this region towards the southern one.

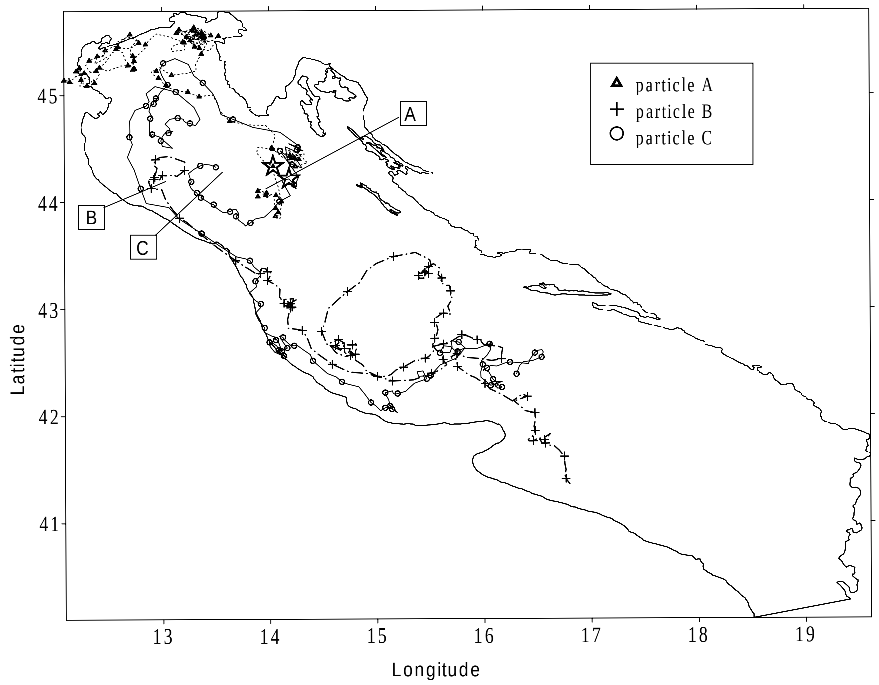

Fig. 7. – Three numerical drifters tracks shown every seven days: Particle A (triangle, dotted line), particle B (cross, dash-dotted line), particle C (circle, continuous line). Particle B is released in January when A and C, released in December, are in the position signed with a large star.

The drifters have the tendency to accumulate mainly along both the western and eastern coasts [31] especially in the central and southern region. The western flow directed southward is more intense and concentrated in a boundary layer along the Italian coast, while the eastern current, pointing northward, is wider. Interesting meanders with a 10–15 days scale are highlighted by drifter trajectories, one aspect where this approach could provide useful hints to sub-grid parameterization.

During winter time of Run 1, as expected, dense water is formed mostly in January and February, with an amount increasing year by year. From the vertical point of view, Run 1 therefore generates an antiestuarine cell. Density transects along the main axis of the basin show that in autumn the upper thermocline is broken and the mixing, consequence of cooling, homogenizes the entire water column in the northern region. In this area the strong winter cooling imposed originates a dense-water formation as shown by the outcropping of isopycnals. This tendency becomes more evident during winters, leading to water masses more and more dense from year to year [30]. As an example of the vertical structure, we can see, on fig. 8, the density anomaly (average relative to the last 15 days of February of 5th year, Run1) along the major axis of the Adriatic Sea (transect B-A, see fig. 1 for location). Summer heating stops the process and restores the stratification; water formed during winter flows southward sinking off the Jabuka pit.

Run 2 provides a completely different situation, as the summer heating is more important than the winter cooling. The vertical circulation established is now estuarine and an anticyclonic horizontal circulation is generated. Only during the first winter there is a

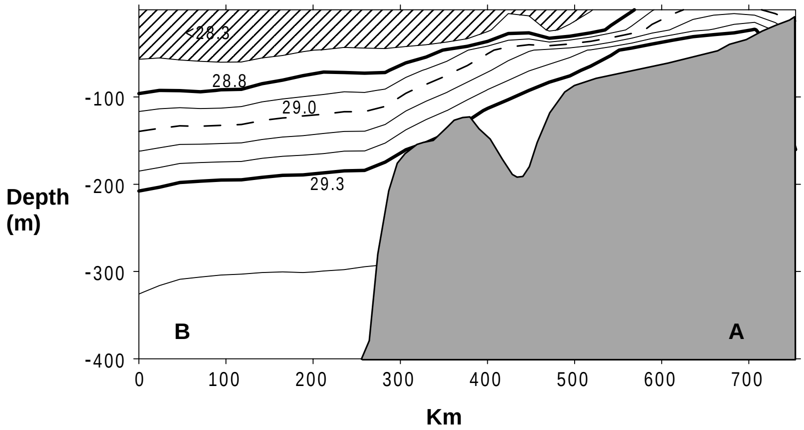

Fig. 8. – Values of density anomaly (kg/m^3) along the direction B-A (see fig. 1), average relative to the last 15 days of February in the 5th year.

dense-water formation on the northern basin, due to the memory of the initial conditions imposed; then the summer strong heating warms up the water in this shallower region, forming lighter water. The stratification produced remains stable even during following winters.

The general behaviour of Run 3 is similar to that of Run 1; again, the winter cooling determines homogenisation and bottom water formation, but a stronger summer heating causes: a) a more intense flushing of the northern region; b) a southward "sliding" of the new water formed; c) a much more efficient turnover of the Jabuka pit and d) the spreading of dense water in the southern basin. Therefore, the quantity of dense water does not increase during the simulation as happened in Run 1, and the kinetic energy remains almost equal to the value of the first year (fig. 3).

After having defined V_{formed} as the dense-water volume formed in the basin that has reached Jabuka pit, and V_{pit} as the pit volume itself, the ratio $R_{\text{vol}} = V_{\text{formed}}/V_{\text{pit}}$ has been computed for all the Runs, and its value is shown in fig. 9. In Run 1 (faint line) the amount of dense water with a density anomaly of 29.3 kg/m^3 increases every year, and in three years the Jabuka pit seems completly filled with this water mass (*i.e.* the volume fraction in fig. 9 reaches the value of unit). It is interesting to note that there might be a volume of dense water related to the hydrodynamic stability of the water column, roughly equal to about 1/5 V_{pit}. The remaining amount of dense water present in the pit and produced in the first year (*i.e.* the fraction of the line above 1/5 during the first year) can be compared to the volume exported during the fifth year, indicated by a thick line in fig. 9. This estimate means that, by adopting the heat fluxes of Run 1, most of the dense water stored requires at least 5 years to leave the pit. In Run 2 the volume of water with density anomaly of 29.1 kg/m^3 decreases rapidly after the first year, the pit is not filled up with dense water and a steady-state condition is reached after three years. In Run 3, no evident changes occur on the R_{vol} value computed for dense water equal to 29.3 kg/m^3 in five years, and in two years the system reaches a steady state. The filling of the pit is not reached even if, as observed in Run 1, the volume of dense water is always greater than 1/5 of the pit volume, meaning that the water flushing with the

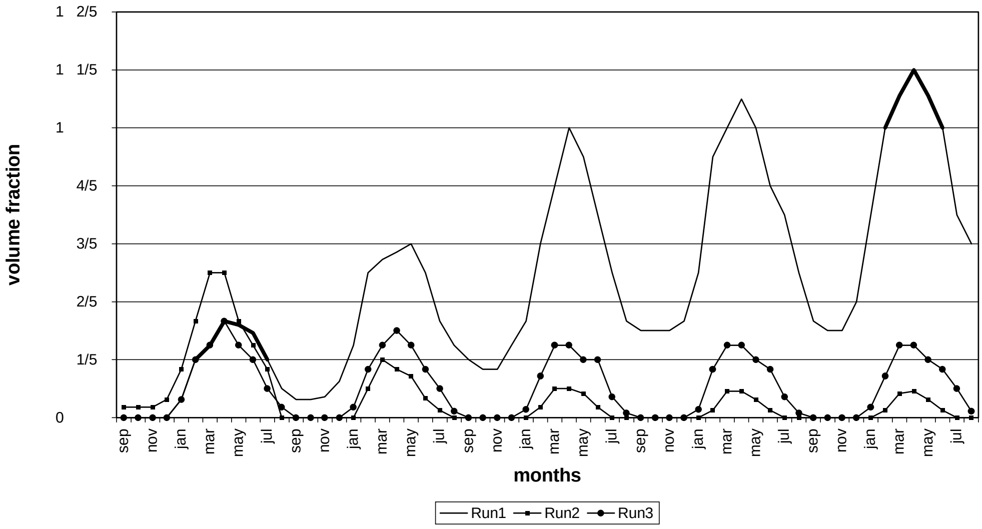

Fig. 9. – Evolution of $R_{\rm vol}$ ratio during the three experiments. The continuous thick line could be considered as the volume exported in Run 1.

surface heat fluxes adopted in this run is more efficient and more water of the sub-basin water is "drained".

3˙2. *Turnover of the Jabuka pit.* – The residence time of bottom water in the Jabuka pit (fig. 1) and the flushing of the northern region are then strongly influenced by the heat fluxes imposed. The turnover times of the water column are very different in the three experiments and results are partially counter-intuitive.

In Run 1 the strong winter cooling (negative annual heat balance) produces a large amount of dense water [32] while the summer heating is not enough to generate a strong circulation able to completely drain the remaining water stored on the bottom of the pit. In this condition, every year some additional denser water would be required to allow the turnover of the pit. As expected, Run 2 residence time gets also larger, even if it is because no significant dense-water formation occurs. On the other hand, it is interesting to note that in Run 3, when the annual balance of heat fluxes is negative but close to zero, the dense-water residence time in Jabuka pit is minimum and therefore the water exchange rate is higher than that of the other two experiments.

This means that a more efficient flushing, with respect to Run 1, is induced by the high summer heating, and the dense water produced in the winter time flows away from the Jabuka pit more rapidly. The dense water formed upon the shelf and driven to the pit has a shorter turnover time in this experiment, meaning that water is not stored for a long time and the renewal is faster than those obtained with the two other experiments.

4. – Conclusions

This work was focused both on the vertical thermohaline circulation and on the horizontal general one of the Adriatic Sea, induced only by the heat fluxes between the sea and the atmosphere as a forcing mechanism.

Three numerical experiments examining the generation and evolution of the thermohaline circulation and its relatively (induced) turnover time in the mid-Adriatic pit, induced by different heat fluxes evolutions, have been carried out. Despite the use of a coarse-resolution grid and a relatively idealized (even though realistic) flux behaviour, the adopted model provided interesting results.

Surface heat fluxes having negative annual budget (Run 1, $-21.6\ \mathrm{W/m^2}$), imposed perpetually every year, are able not only to start a dense-water formation process and a generally cyclonic circulation, but an antiestuarine vertical circulation and a long turnover time of the Jabuka pit as well. The adopted fluxes can represent a situation similar to a "cold year" (in agreement with estimations made by other authors [20, 24, 25, 32, 33]).

If the annual heat fluxes are slightly positive (Run 2, $8.3\ \mathrm{W/m^2}$), a situation representing a possible "warm year", there is no evidence of dense-water formation. The vertical circulation established in the northern sub-basin is estuarine, while the horizontal one is anticyclonic. A strong vertical stratification exists during the year as the winter cooling event is not sufficient to generate dense water and to induce the vertical mixing. In this way the northern Adriatic flushing occurs from the intermediate or bottom layers and the water column under the thermocline cannot be ventilated; consequently, some deep water masses can remain isolated.

In the third experiment the annual heat fluxes budget is slightly negative (Run 3, $-7.5\ \mathrm{W/m^2}$), thermohaline circulation is antiestuarine, but in this case there is almost a balance between the dense water formed during the winter time and the summer flushing, in a way that the Jabuka pit turnover time diminishes. This experiment is an intermediate situation between the two previous ones, and the most sensitive to a minimum variation of the fluxes, able to switch the circulation from antiestuarine to estuarine in relation to a natural interannual variability.

The heat fluxes interannual variation can involve an oscillation in the northern-central Adriatic Sea between the situation observed in Run 1 and Run 3, thus a shifting between years of dense-water formation and others characterized by a more efficient flushing.

The results of this work pointed out that in the northern Adriatic region, by prescribing only the heat fluxes, a horizontal and vertical general circulation can be generated, similar to the experimentally observed one. This raises interesting questions about the mean wind field effects on the basin circulation, which could be more important in modulating—rather than generating—long time features of the currents, and may become more relevant on relatively short time scales; on the other hand, it could be possible that, for longer time scale processes, heat fluxes changes may influence the general circulation more than winds.

The fluctuations between colder years (negative annual heat balance) and warmer ones (annual heat balance close to zero) are of primary importance for the climatic state of the area and for the efficiency in flushing the northern semienclosed basin; indeed, they may allow the system to evolve without an increment of energy, which, on the contrary, would be necessary if a sequence of cold years would lead to more stratified conditions.

* * *

The work was supported by Co.Ri.La. Project 3.1 (U.O. 2, CNR-ISDGM, `http://www.corila.it`).

REFERENCES

[1] Mork K.A. and Skagseth O., *Climate Dynamics*, **12/10** (1996) 737.
[2] Schlesinger M. E. and Ramankutty N., *Nature*, **367** (1994) 723.
[3] IPCC (2001). *Climate Change 2000. The Science of Climate Change. Contribution of working group I to the third assessment report of the Intergovernmental Panel on Climate Change* (Cambridge University Press, Cambridge) 2001.
[4] Manabe S. and Stouffer R. J., *Nature*, **364** (1993) 215.
[5] Cai W., *J. Geophys. Res.*, **101-C1** (1993) 1079.
[6] Seidov D., Barron E. and Haupt B. J., *Global and Planetary Change*, **30** (2001) 257.
[7] Stratford K. and Haines K. , *J. Marine Systems*, **33-34** (2002) 51.
[8] Hulme M., *et al.*, *Global and Environmental Change*, **9** (1999) S3.
[9] Rosenzweig C., *Climatic Change*, **4** (1985) 239.
[10] White A., Cannell M. G. R. and Friend A. D., *Global Environmental Change*, **9** (1999) S21.
[11] Santer B. D. *et al.*, *J. Geophys. Res.*, **100-C6** (1995) 10693.
[12] Bergamasco A. Oguz T. and Malanotte Rizzoli P., *J. Marine Systems*, **20** (1999) 279.
[13] Artegiani A. *et al.*, *J. Phys. Oceanogr.*, **27** (1997) 1492.
[14] Artegiani A. *et al.*, *J. Phys. Oceanogr.*, **27** (1997) 1515.
[15] Mellor G. L., *User guide for a three dimensional, primitive equation, numerical model. Progress in Atmosphere and Ocean Science* (Princeton University) 1998, `http://www.aos.princeton.edu/WWWPUBLIC/htdocs.pom`.
[16] Mellor G. L. and Yamada T., *Rev. Geophys. Space Phys.*, **20** (1982) 851.
[17] Bergamasco A., Carniel S., Pastres R. and Pecenik G., *Estuarine, Coastal and Shelf Science*, **46** (1998) 483.
[18] Zavatarelli M., Pinardi N., Kourafalou V. H. and Maggiore A., *J. Geophys. Res.*, **107-C1** (2002) 4/1, doi:10.1029/2000JC000210,2002.
[19] Shapiro R., *Rev. Geophys. Space Phys.*, **8** (1970) 359.
[20] Polli S., *Atti del IX° Convegno dell'Associazione Geofisica Italiana* (1960) 1.
[21] Bergamasco A. and Gacic M., *J. Phys. Oceanogr.*, **26** (1995) 1354.
[22] May P. W., Naval Ocean Research and Development Activity, Rep. 54, NSTL, MS 39529, (1982).
[23] Artegiani A., Cushman-Roisin B., Gacic M. and Poulain P. M., *Physical Oceanography of the Adriatic Sea. Past, Present, Future* (Kluwer Academic Publishers) 2002.
[24] Stravisi F. and Crisciani F., *Boll. Oceanol. Teor. Appl.*, **4** (1986) 55.
[25] Picco P., *Nuovo Cimento C*, **14** (1991) 335.
[26] Orlic M., Gacic M. and La Violette P. E., *Oceanol. Acta*, **15** (1992) 109.
[27] Carniel S. *et al.*, *Science & Justice*, **42** (2002) 143.
[28] Poulain P. M., *J. Marine Systems*, **20** (1999) 231.
[29] Poulain P. M., *J. Marine Systems*, **29** (2001) 3.
[30] Malanotte-Rizzoli P., *Atti Istituto Veneto di Scienze, Lettere ed Arti, Venice* (1994), p. 268.
[31] Franco P. *et al.*, *Oceanol. Acta*, **5** (1982) 379.
[32] Hendershott M. C. and Rizzoli P., *Deep-Sea Res.*, **23** (1976) 353.
[33] Maggiore A., Zavatarelli M., Angelucci M. G. and Pinardi N., *Phys. Chem. Earth*, **23** (1998) 561.